Model for the Excitation Dynamics in the Light-Harvesting Complex II from Higher Plants

Gediminas Trinkunas, James P. Connelly,† Marc G. Müller,† Leonas Valkunas,‡ and Alfred R. Holzwarth*,†

Max-Planck-Institut für Strahlenchemie, Stiftstrasse 34−36, Mülheim a.d. Ruhr, D-45470, Germany, and Institute of Physics, Vilnius 2600, Lithuania

Received: December 3, 1996; In Final Form: April 1, 1997[⊗]

A model for the spectral characteristics, the transition dipole moment orientations, and the energy transfer properties of chlorophyll (Chl) *a* and *b* molecules in the light-harvesting complex (LHC) II is proposed on the basis of the results from femtosecond transient measurements and other spectroscopic data. The model uses the structural data (Kühlbrandt; *et al. Nature* **1994**, *367*, 614) and is obtained using a genetic algorithm search of the large parameter space. Förster resonance transfer has been assumed as the mechanism of energy transfer. The spectral and orientational assignments of all twelve Chl molecules of a LHC II monomer are proposed. In the best fit model two of the seven Chl molecules that are proximal to the central luteins are Chl *b*. In contrast to prior assumptions, the basic feature of the model consists of an intermediately strong coupling ($V < 100$ cm^{-1}) between the Chl *a* and *b* molecules in close pairs and the absence of substantial excitonic coupling between Chls *a*, thus indicating an overall limited influence of excitonic effects on spectra and kinetics. A theoretical estimation of exciton effects supports these model assumptions. Over most of the difference absorption spectrum good agreement between experimental and theoretical kinetics has been obtained. Energy transfer times in the symmetric LHC II trimer range from 90 fs to 5.1 ps. For the monomeric complexes only the longest lifetime is significantly affected and predicted to be just slightly longer (6.6 ps). The predicted transition dipole moment orientations result in weak coupling between the LHC II monomers. Several possible routes to improve both the data fitting and the reliability of the predictions in the future are discussed.

Introduction

The recently resolved structure of the major light-harvesting antenna complex (LHC) II[1] from higher plants has motivated substantial efforts to understand the mechanism of light harvesting in higher plant photosynthesis. This pigment−protein complex is the outermost and most abundant light harvesting antenna of photosystem II.[2] It shows the same structural motif as the minor inner complexes CP24, CP26, and CP29 and is also homologous to LHC I of photosystem I.[3] The complex contains at least five chlorophyll (Chl) *b* and seven Chl a chromophores per monomer. By studying the excitation energy transfer routes in this complex and analyzing them on the basis of accepted physical theories, it is hoped to eventually understand on a molecular level a variety of problems, such as non-photochemical quenching mechanisms,[4] the mechanism for preventing chlorophyll triplet formation,[5] the role of carotenoids, and others. At present the structural data leave open a number of important details, such as the orientation of transition dipole moments, the spectral assignment of Chls, and, even more importantly, the assignment of Chl *a* and Chl *b* to specific pigment positions in the complex. Furthermore the location of at least one carotenoid molecule is still missing in the structure.

The center of the complex is formed by two x-crossed lutein molecules. This has led to the hypothesis that Chl *a* molecules should be situated in close contact to the luteins and Chls *b* should be located at the periphery, i.e., further away from the luteins. Thus carotenoid molecules could efficiently quench the triplet states that are expected to be preferentially formed on Chls *a*.[1] It is important to realize that even with exact structural information, providing the full assignment of Chls, most problems related to the functioning of the complex would remain unsolved.

Much steady state and kinetic spectroscopic work has been performed with the aim of identifying and assigning the spectral properties of individual Chl molecules and to establish the time scales of energy transfer between them. In particular, the absorption and circular (CD) and linear dichroism (LD) data obtained at low temperatures have revealed a variety of spectral forms[6] that are close to the number of pigments present in a LHC II monomer (the usually studied aggregation form is a trimeric complex). Recent steady state spectroscopic data, in combination with a model calculation for exciton coupling, provided the first data on the possible transition dipole directions for several Chl molecules.[7] A number of kinetic studies have established chl energy transfer kinetics.[8−13] Eads *et al.* first observed subpicosecond Chl *b* to Chl *a* transfer;[11] Kwa *et al.* were the first to accurately measure the 5 ps component.[14] Subsequent studies have reported an additional faster Chl *b* to Chl *a* energy transfer component,[10,17,18] as well as various picosecond (5,[8−10,14,17,18] 10−30,[8,10,12−15] and 100−200 ps [14,15]) kinetic components reflecting Chl *a* to Chl *a* energy transfer (5 ps), and possible annihilation and quenching processes. Using the transition dipole orientations defined from the excitonic model,[7] a recent pump−probe femtosecond kinetic study performed at 77 K found no discrepancy with the current hypothesis concerning the Chl *a/b* assignment.[1] However, the assignment of kinetic components to individual Chl molecules is problematic for various reasons. Firstly, many quite dissimilar arrangements or pigment orientations and assignments may result in very similar theoretical kinetics. Secondly, the problem is compounded further by the fact that in most of the work cited above the excitation conditions led to partial excitation annihilation. Due to the dissipation of excess energy during the

* Author to whom correspondence should be addressed. Fax: (+49) 208-3063951. E-mail address: holzwarth@mpi-muelheim.mpg.de.
† Max-Planck-Institut für Strahlenchemie.
‡ Institute of Physics.
⊗ Abstract published in *Advance ACS Abstracts,* August 15, 1997.

S1089-5647(96)03968-5 CCC: $14.00

annihilation process, an alteration of the pigment spectral properties cannot be excluded.[16]

Essentially annihilation-free femtosecond transient absorption measurements performed recently on trimeric complexes of LHC II[17] provide a new basis for correlating the available structure data with spectral as well as kinetic information. Moreover, the extension of these very low intensity measurements to excitation in the carotenoid absorption region (470−515 nm)[18] provided the first direct evidence that some Chl *b* molecules are the primary excitation acceptors from the excited luteins and are thus probably located in close proximity to luteins, in contrast to the currently accepted hypothesis. This argues against the current Chl *a/b* assignment and inspired us to perform kinetic simulations of excitation dynamics using genetic algorithms similar to those performed for the PS I core complex.[19,20] This approach has a number of advantages. It allows us to test a huge number of models with different spectral type and transition dipole orientation distributions (more than 10^5 per run) and to reveal the trends showing up in different models. Our main aim is to assign individual Chl spectral forms (based on the molecular Chl spectrum in ether) and transition dipole moment orientations to specific pigment sites in the structure. To achieve this, we search for the best fitting simulation of the annihilation-free transient absorption data.[17] We also incorporate into the search various steady state spectroscopic properties, including LD. Our simulations support the experimental evidence[18] that some Chl b molecules should be located in close contact to the luteins and provide further arguments against the currently postulated Chl *a*/Chl *b* arrangement.

In the following sections we briefly describe the modeling procedure, and then we discuss the assumptions made and the initial parameter set used for the simulations. Finally the simulation results and their relation to other available data will be presented and discussed.

Modeling Procedure

Model Assumptions. The aim of the simulations is to find the detailed assignment of individual spectra and orientations to specific Chl molecules in the structure on the basis of the room temperature transient absorption data.[17] This problem is in principle analogous to simulations we performed previously when modeling the fluorescence decay kinetics in PS I core particles.[19,20] Our approach is based on the assumption that the absorption spectrum of the LHC II trimer can be described as being composed of the sum of the 12 individual Chl molecule spectra (5 for Chls *b* and 7 for Chls *a* per monomer). For our approach validity of the Förster mechanism is assumed; i.e., we do not consider any exciton coupling effects other than (limited) spectral shifts. This basic assumption of the model will be justified below also on theoretical grounds. The particular spectral type and transition dipole moment distributions are then used to define the initial excitation conditions for the energy transfer within the LHC II structure. The excitation decay is calculated using the Pauli master equation (see Appendix A), and it is compared to experimental transient absorption decay curves at all available probe wavelengths in a global fit procedure. A χ^2 type criterion[20] is used to judge the fitness of a particular model (see eq 1). Since experimental data were obtained under isotropic measurement conditions, the C_3 symmetry of the LHC II trimer[21] can be exploited to reduce the dimension of the transfer rate matrix in the Pauli master equation (see Appendix A).

Importance of Excitonic Effects. An important problem with regard to the concept of this paper and the choice of the model is the question to what extent exciton coupling effects influence the spectroscopy of LHC II. From the structure it appears likely that there exist several closely spaced Chl *a* and/or Chl *b* pairs. With application of a point dipole approximation to the structure and a refractive index $n = 1.34$, candidates for strong coupling could be the pairs (using the notation of ref 1) *a*2−*b*2; *a*3−*b*3, *a*5−*b*5; *a*6−*b*6[1] in the case of favorable transition dipole moment orientations. Their couplings, if strong, would give rise to characteristic excitonic splitting of absorption spectra and influence the excitation decay kinetics on the femtosecond scale, possibly also giving rise to oscillatory features. From the structure, maximal coupling energies V can be estimated to be approximately 100 cm^{-1}, for optimal orientation of transition dipole moments. While the splitting in the absorption spectrum could hardly be seen due to the strong inhomogeneously broadened absorption spectra which is of the same order of magnitude, the almost conservative CD spectrum of LHC II in the Chl *a* absorption region[22] could be evidence for excitonic effects. The interpigment coupling of about 90 cm^{-1} as estimated from the CD spectrum[22] could serve as a measure for the coupling strength of some Chl pairs and for expected coherence effects. If such pairs of strongly coupled Chl molecules would appear as a result of the simulation, this would impose the requirement for an iterative procedure for the spectral decomposition, i.e., further simulation runs based on an improved spectral decomposition for every step, accounting for the excitonic effects for the particular pairs of strongly coupled molecules. Such iterations would eventually provide a self-consistent description of LHC II steady state and transient spectral properties.

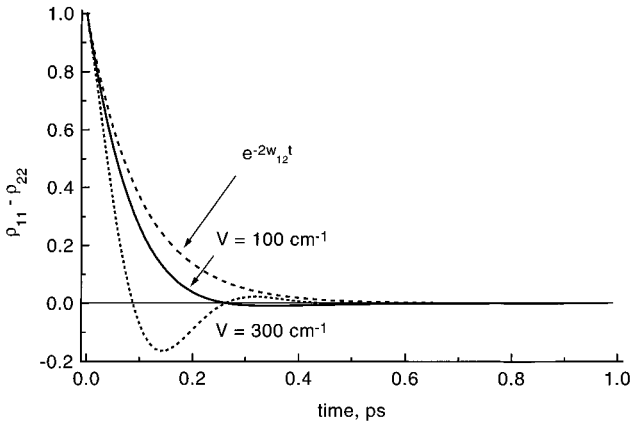

Figure 1. Coherent vs incoherent excitation equilibration kinetics in a degenerate dimer. *Solid* and *dotted* lines show the decays of the diagonal density matrix element difference calculated using the stochastic Liouville equation approach.[23] The parameters used are as follows: incoherent part of intradimer hopping rate (Förster transfer rate) $w_{12} = 5$ ps^{-1}; off-diagonal density matrix element decay rate $\Gamma = 6.2$ ps^{-1} (∼210 cm^{-1}); intermonomer coupling energy $V = 100$ cm^{-1} (*solid* line) and 300 cm^{-1} (*dotted* line). *Dashed* line shows the decay of monomer occupation difference $\rho_{11} - \rho_{22} = \exp(-2w_{12}t)$ due to kinetic balance equations (eq B1 for $V = 0$) with the Förster transfer rate w_{12} as indicated above (see Appendix B).

The effect of strong coupling between pairs of Chl molecules on the excitation decay kinetics can be roughly estimated by using the stochastic Liouville equation approach for a degenerate dimer.[23] In Figure 1 we show the expected phase equilibration kinetics in a degenerate dimer, taking into account the excitation phase coherence following this approach[23] (see also Appendix B). Comparison of the equilibration kinetics predicted by simple occupation balance equations with the same interpigment Förster transfer rate shows that at a coupling energy of $V = 100$ cm^{-1} both decay curves are rather close without showing any pronounced oscillatory features. The difference between the decay curves is further substantially reduced when the monomer energy levels are not equal, as would be the case in, e.g., Chl *a/b* pairs. In conclusion, at the coupling strengths expected in

TABLE 1: Parameters Defining the Spectral Shape of a Single Chl Molecule Absorption[a]

band	amplitude	shift (cm^{-1})	fwhm (cm^{-1})
1	60.2	0	285
2	25.8	100	510
3	13	1160	751
4	6.7	2310	706
5	3.6	3690	1326

[a] The spectrum is composed by five Gaussian bands[24] obtained by decomposing the absorption spectrum of Chl *a* in ether solution. All bands were narrowed by about 14%, and the Stokes shift was varied to find simultaneously the best fit of the LHCII absorption and steady state fluorescence spectra. The corresponding fluorescence spectra were calculated from the absorption using the mirror relationship. The optimal Stokes shift was found to be 80 cm^{-1}. Chl *b* was assumed to have 61% of the spectral amplitude of Chl *a*.

the LHC II complex there probably exists essentially no possibility to distinguish on the basis of isotropic absorption decay measurements between the two energy transfer mechanisms. The pronounced coherence effects show up only when the coupling energy V is increased by a further factor of about 3. Since the couplings in the hypothetical candidate dimers of LHC II, as estimated from the structure and possible optimal orientations, never exceed the value estimated from the CD spectrum ($V \sim 90$ cm^{-1}), we feel sufficiently justified to describe energy transfer in LHC II in the present model calculations exclusively by the Förster mechanism. This does not exclude, however, that some band shift effects have to be taken into account or that some other consequences of weak excitonic coupling could become important. The role of such effects needs to be explored by further experiment. Despite our assumption in this paper we definitely do not entirely exclude the relevance of some limited excitonic coupling effects. With our basis of Förster energy transfer and relatively weak pigment coupling, we do not try to fit the CD spectrum which, although more sensitive to the coupling between pigments, is also complicated by other effects. Firstly, the experimental CD spectrum at room temperature is not conservative, and the precise origin of this effect is not known. On the other hand our calculated excitonic CD spectrum would be conservative by definition. Secondly, dynamic effects are also important. The calculated CD spectrum is for example very sensitive to small Chl plane orientation changes; the chlorin ring breathing mode has an amplitude of about 0.05 nm, and the calculated CD spectrum should account for this by averaging over the plane orientation distribution. Thirdly, on the wavelength scale just the red region is relatively clearly defined in its origin. The blue part is formed of the Chl *b* band with Chl *a* vibration subbands superimposed. The CD spectrum in the vibrational subband region is an open topic. Scherer and Fischer, for example, made quantum chemical transition dipole moment orientation calculations for BChls in the reaction center. They found that the transition dipole orientations differ from the line connecting the nitrogen atoms. Moreover, the transition dipoles are out of the BChl plane. All of these points strongly argue against putting any relevance at present into a single-minded CD calculation, and consequently we do not include such data in this paper despite the fact that we have calcuated all of these data along with the simulations.

Parameters for the LHC II Model. All theoretical absorption spectra of individual Chls were assumed to have the same shape, given by a five Gaussian band approximation of the Chl *a* absorption spectrum in ether[24] with ~14% band narrowing but keeping the Chl *a*/Chl *b* amplitude ratio 1.64.[25] The parameters of the Gaussian bands used in the present study are shown in Table 1 and are the same as those used in refs 19 and 20. The spectral maxima for the Chl absorption bands were found by decomposing the LHC II absorption spectrum at room temperature into 12 bands (5 bands for Chl *b* and 7 for Chl *a*; see Figure 2) with the only additional restriction that Chls *b* should have maxima below 660 nm. Fixing the Stokes shift, assumed to be the same for all forms, the mirror image relationship was used to calculate the individual Chl fluorescence profiles, taking into account the necessary corrections for wavelength dependence.[26] The individual absorption−fluorescence symmetry point (frequency scale) defines the individual Chl excitation energies (energy E_j used in eq A3, Appendix A). The Stokes shift, assumed to be the same for all of the spectral forms, was determined to be 80 cm^{-1} from the requirement to fit simultaneously the experimental steady state fluorescence spectrum of the LHC II trimer (see Figure 3 and Table 1) with the theoretical spectrum for the thermally equilibrated Chls in the complex. The obtained individual absorption and fluorescence spectra of Chl molecules were subsequently used to calculate the overlap integrals for Förster transfer rates[28] which define the transfer matrix in the Pauli master equation (see Appendix A). This procedure in itself already ensures the validity of the detailed balance relationship. In addition we only calculated the downhill rates (in energy) between Chl pairs by the Förster formula, whereas the uphill rates were calculated from the Boltzmann relationship.

In order to fit the calcualted transient absorption kinetics to the measured one, the difference absorption spectrum of each

TABLE 2: Effect of Intermonomer Coupling on the Lifetime Values in LHC II Trimers[a]

lifetime component *i*	monomer lifetime τ_i (ps) (rel amplitudes (a_i))	trimer lifetime τ_i (ps) (rel amplitudes (a_i)
1	3600 (0.52)	3600 (0.52)
2	6.6 (0.15)	5.1 (0.15)
3	3.5 (0.01)	3.0 (0.01)
4	1.8 (0.17)	1.7 (0.17)
5	1.6 (0.13)	1.4 (0.13)
6	1.2 (0.19)	1.2 (0.19)
7	0.50 (0.21)	0.47 (0.21)
8	0.34 (0.05)	0.32 (0.03)
9	0.31 (0.21)	0.3 (0.20)
10	0.26 (0.16)	0.24 (0.11)
11	0.21 (0.18)	0.21 (0.18)
12	0.09 (0.32)	0.089 (0.32)

[a] The monomer and trimer lifetimes τ_i are calculated for the same spectral type and transition dipole moment distribution obtained in the free search (see Table 3). In parentheses are given the relative amplitude values (a_i) at the maximum of the corresponding DADS.

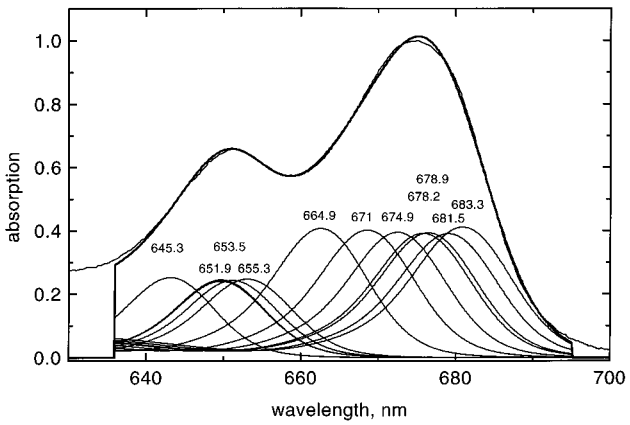

Figure 2. Decomposition of the absorption spectrum of the LHC II trimer (thin line) into 12 Chl spectral forms. The numbers near the absorption maxima indicate the zero phonon line positions on the wavelength scales. The form of the individual absorption spectrum is described in Table 1. The Chl *a* and Chl *b* amplitude ratio (1.64) is used from the corresponding absorption spectra in ether.[25] The amplitudes of all the Chl molecules are multiplied by 2 for better presentation.

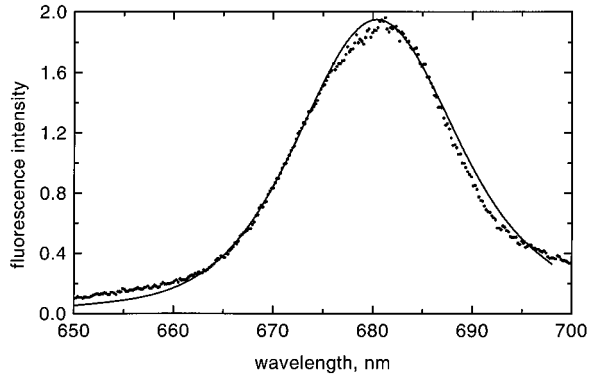

Figure 3. Expedrimental (solid circles) and calculated (solid line) steady state fluorescence spectra of the LHC II trimer at 298 K. The latter was obtained from the sum of the individual Chl fluorescence spectra weighted by corresponding Boltzmann factors. Fluorescence spectra have been obtained from absorption spectra using the mirror image relation. Fit of the spectra was obtained by varying (to the same extent) the widths of Gaussian subbands and the Stokes shift.

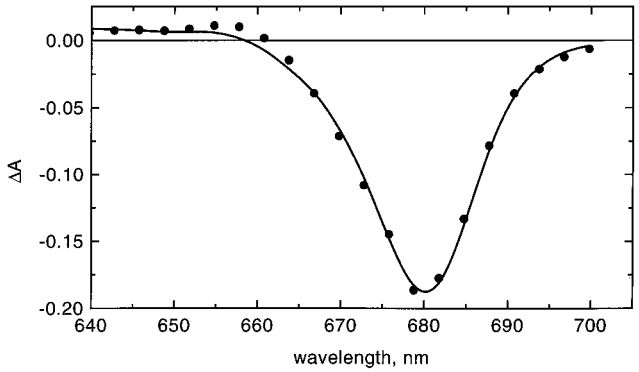

Figure 4. Experimental 3.6 ns component DADS (solid circles) compared with the theoretical one (solid line) obtained from the model spectra by summing the various Chl *a*/*b* difference spectra weighted by the corresponding Boltzmann factors.

Chl (SADS)is required also. These were obtained from the experimental Chl *a* and Chl *b* absorption difference spectra in ether.[34] The main bleaching band of these experimental spectra was narrowed (by ~20%) in order to be able to closely describe the experimental long-time (3.6 ns component) absorption difference spectrum, which should be characteristic for the difference spectrum of the thermally equilibrated trimeric complex (see Figure 4). The latter was calculated by shifting the maxima of the individual absorption difference spectra (SADS) to the mirror symmetry point between the respective absorption and fluorescence. This is essentially the same procedure as was employed when the Stokes shift of the fluorescence spectrum was determined (see above).

Assignment of Spectral Type and Transition Dipole Moment Orientation. Once the problem is defined in the manner described above with fixed individual spectra, the task is to assign a specific site and a dipole orientation to each individual Chl. As stated, the number of all possible combinations is finite. Thus, one might consider testing all possible combinations and comparing the results of each simulation to the experimental data. The calculation of one assignment as well as its fitness takes about 0.17 s on our fast workstation. Since there are about 2×10^{12} possible combinations, the direct approach is clearly unfeasible and an efficient search algorithm is required. We used a genetic algorithm implementation[27] to carry out the search as described previously.[20] The spectral types were represented by a string of 12 byte labels and the 12 orientations of transition dipoles by a 12 bit string (0 stands for the vector connecting the opposite nitrogen atoms of Chl molecule starting from the atom with the lowest number of a given tetrapyrrole ring in the protein database file; 1 stands for the perpendicular direction). A further problem needs to be solved simultaneously in order to arrive at an optimal fitting: the expression for the Förster rate[28] contains the refractive index *n*, which is unknown but has a significant influence on the rates. We introduce *n* as an additional free fitting parameter which is represented by a bit string. A single *n* was assumed to be valid for all Chl pairs.

A starting population (*N* individuals) was created at random, and the Pauli master equation was solved for each individual. Then the fitness was calculated, defined by

$$F = \left[\frac{1}{N_{\text{exp}}} \sum_{i=1}^{N_{\text{exp}}} \frac{(x_i - x_i^{\text{exp}})^2}{x_i^{\text{exp}}} \right]^{-1} \quad (1)$$

where x_i and x_i^{exp}stand for the calculated and experimental time points of the kinetics at each wavelength, respectively, and N_{exp} is the number of data points to be compared. Next, pairs of individuals were chosen at random for "crossing-over", which means that randomly selected parts of strings in these pairs are swapped to create two offsprings with combined "genes" for a new generation. Furthermore a small part of the strings undergoes a random mutation with a low probability. This procedure ensures a higher degree of diversity in the population and avoids trapping in a local minimum. Then, the next generation is created until the maximum number of preselected generations is reached. A full description of the genetic algorithm used may be found in ref 20.

Testing of the Procedure. The procedure was tested on synthetic data in order to estimate the robustness and suitability of the method concerning the present problem. Synthetic kinetics with 12 components (lifetimes and decay associated difference absorption spectra—DADS) were generated for randomly distributed spectra and transition dipole moment orientations of an LHC2 trimer. Data points between 640 and 700 nm at intervals of 3 nm were used as input data in the test procedure. The test runs showed that the search procedure was unable to unequivocally determine the input distribution. The main reason is that the initial excitation conditions simulating the experimental conditions (excitation wavelength 650 nm and 12 nm spectral width of the exciting 70 fs pulse) already produce an excitation distribution that is partially equilibrated, as one can see from the relatively small amplitudes of equilibration kinetic components. As a consequence, many different arrangements yield kinetic curves which are quite similar. Assuming for example 5% errors in amplitudes of kinetic input data, this procedure alone is not capable of unequivocally distinguishing between the correct input distribution and many other, though similar in terms of Chl assignment, solutions. Thus, a further selection criterion is required. We introduced the LD calculation (see AppendixC) as a further important selection criterion that can critically distinguish between different otherwise similarly good solutions for the kinetics. Our simulations clearly show that the differentiation between various similarly good solutions could be highly improved if data with more selective and/or multiple wavelength excitations were used. This will be tested in the future.

Results and Discussion

Pigment Orientation and Spectral Assignment. Search runs were performed for two different models: a restricted model where the Chls *a* can reside only in the vicinity of the luteins,[1] thus testing the current hypothesis on the Chl *a*/*b* localization, and second, a completely free model where Chls *a* and *b* can occupy any site in the structure. As an additional

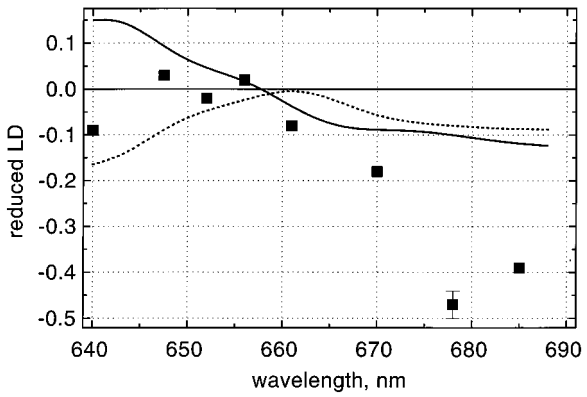

Figure 5. Reduced LD spectra for LHC II trimers. The solid squares (and error bars) indicate experimentally determined points from Table 1 of ref 29 for the average dipole moment orientations after correction for the trimer orientation in the compressed gel. The best fit model obtained with a free spectral type distribution search and with the constrained model suggested by Kühlbrandt *et al.*[1] are indicated by solid and dotted lines, respectively. Models were selected that have the highest fitness and the closest reduced LD values in Chl *b* and *a* regions to about 0, and −0.3, respectively.[7,29] For the definition of reduced LD see Appendix C.

criterion for selecting individuals in the mating pool and for judging the success of the model, we make a qualitative comparison with the LD spectrum.[7,29] Since we do not fit the spectrum, we used only the correct sign, but not the magnitude, of the LD spectrum in the Chl *a* absorption region in addition to a good fit of the kinetics to pick the best solutions in the final generation. It should be noted that the values of LD quoted in this paper and ref 7 refer to the linear dichroism of the trimer pigments in perfectly aligned trimers. These are related to the experimental values in ref 29 by a divisive factor of −0.114,[29] which reflects the orientation of the trimers in the gel used to align the LHC II complexes (see Appendix C).

In the final search runs we used a population of 1000 individuals. The fitness for the best individual of the population generally converged in about 60 generations for both constrained and free models. The fitness for the kinetics of the restricted model was somewhat less favorable (5%) than the one for the free search model. The choice of LD limitation, i.e., the reduced LD values in the Chl *b* and Chl *a* regions of about 0 and −0.3, respectively,[29] were critical in selecting the best solutions and in narrowing down the number of possible solutions. The LD spectrum for the best fit solutions closest to the LD criteria[29] are shown in Figure 5 for both models together with values determined from experiment.[29] No model with good fit to the kinetics could be obtained with LD ≤ −0.15 in the Chl *a* region and more close to zero in the Chl *b* region. However, qualitatively the LD calculated for the optimal free model is in substantially better agreement with the experiment than that obtained for the restricted model. In Table 3 the Chl molecule assignments and transition dipole moment orientations are presented for the best solutions of both models and are compared to the current suggestions.[1,7] Interestingly, the pigment orientations of both models agree with the predictions from the excitonic modeling.[7] This indicates that both the initial Förster and the excitonic representations converge to the same interpigment coupling. It is characteristic for both obtained spectral type distributions that all except one of the most strongly coupled pairs of Chls are Chl *a*−Chl *b* pairs. Moreover, all the transition dipole orientations are such that they result in maximal coupling in these pairs. The only qualitative difference in that respect between the constrained and the free search models is the relatively strongly coupled pair of Chl *b* molecules *b*1−*b*5 (653.5−655.3 nm) present in the former but missing in the latter model. This coupling, if realized, would alter slightly

TABLE 3: Comparison of Different Chl Molecules Assignments and Orientations in the LHC II Monomer[a]

Kühlbrandt et al.	constrained model	orientations	free search model	orientations for free search model
*a*1	*a*-671	0*	*b*-655	1**
*a*2	*a*-678	1	*b*-652	0
*a*3	*a*-665	1	*a*-675	1
*a*4	*a*-675	0*	*a*-682	0*
*a*5	*a*-679	0*	*a*-679	0*
*a*6	*a*-683	0	*a*-665	0
*a*7	*a*-682	0*	*a*-671	0*
*b*1	*b*-655	0	*a*-683	0
*b*2	*b*-652	1	*a*-678	0
*b*3	*b*-645	1*	*b*-654	1*
*b*5	*b*-652	0	*b*-652	0
*b*6	*b*-654	0	*b*-645	1

[a] In the first column the Chl molecule identities are presented as suggested by Kühlbrandt *et al.*[1]. The second and fourth columns show the corresponding data from the present work for the constrained and the free search models, respectively (Chl identity is assigned by a number reflecting the wavelength of absorption maximum in nanometers). In the third and the fifth columns the optimized transition dipole moments of corresponding models are presented. The 0 stands for the vector connecting the opposite nitrogen atoms of the Chl molecule starting from the lowest numbered nitrogen in a given tetrapyrrole ring as it appears in the LHC II protein database file; **1**, for the perpendicular direction. An asterisk indicates the sites where the orientations agree with the one predicted for the excitonic model.[7] A double asterisk indicates disagreement of the present model prediction with the excitonic model.[7] The optimal refractive indices *n* in the constrained and free search models were found to be 1.47 and 1.54, respectively.

the absorption spectrum in the Chl *b* region. It would influence, however, only the very early stage of the kinetics in the Chl *b* region (∼100 fs range) and therefore can be left out of the present discussion to a first approximation. Both models would indicate the high energy funneling trend of energy transfer in LHC II.

The most strongly coupled Chl *a* pair in the obtained structures is *a*6−*a*7. The estimate of interpigment coupling gives a low value of ∼30 cm^{-1}. Therefore, we do not expect excitonic coupling to considerably alter the absorption spectrum and thus our spectral decomposition. Furthermore, due to weak intramonomer coupling the CD spectrum in the Chl *a* absorption region of the trimer may be expected to originate partially from the LHC II intramonomer as well as to substantial extent from intermonomer coupling.

Two of the Chls *b* (*a*1, 655 nm and *a*2, 652 nm in the notation of ref 1; see Table 3) in the free search model are predicted to be close to the central luteins, in contrast to the suggestion of Kühlbrandt *et al.*[1] This finding is perfectly in line with the recent experiments[18] where excitation of the luteins is followed by sequential bleaching first in the Chl *b* and then in the Chl *a* absorption region. Since the structural assignment of Kühlbrandt is well-documented[1] and discussed in the literature,[7,10] we now discuss further only the alternative best solution from the free search.

Energy Transfer Kinetics. In Figure 6a,b the calcualted DADS are compared with the experimental ones.[17] The 5.1, 0.47, and 0.22 ps lifetimes compare quite well with the experimental 6, 0.48, and 0.18 ps lifetimes, respectively. The corresponding DADS spectral shapes, however, are harder to fit and differ somewhat. The calculated kinetics predicts three additional components, not resolved in the experimental data, of 1.4 ps, 0.31 ps, and 90 fs with considerable amplitudes which reflect complex equilibration processes. In experiment, these components are mixed to result in significantly altered experimental spectra (DADS).

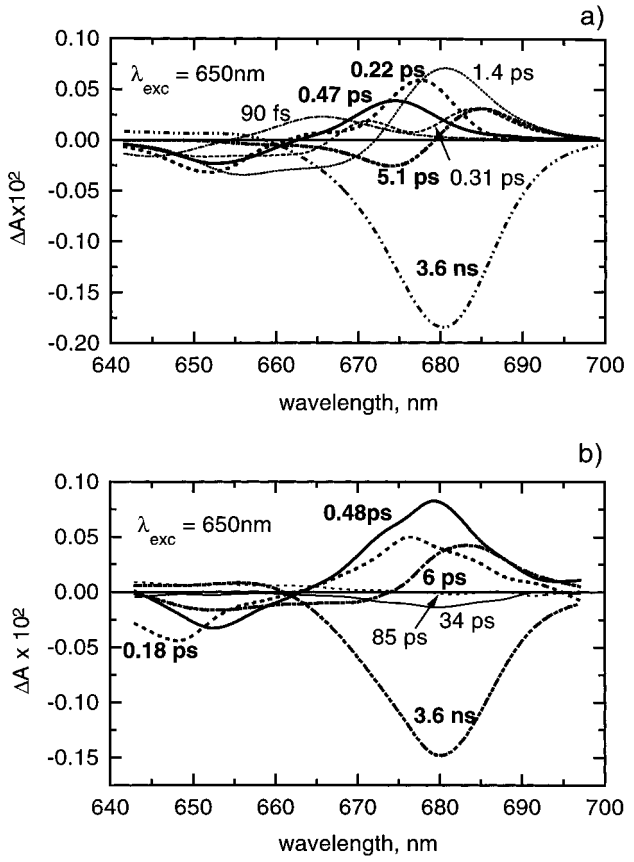

Figure 6. Comparison of the experimental (a) and the DADS calculated for the best fit model from the free search (b). Lifetimes are given as numbers. The bold numbers and thick lines indicate those DADS components that bear the closest similarity to the experimental ones. For details see text.

The experimentally observed 6 ps component seems to reflect the time scale of equilibration between the redmost Chl(s) and the pool of all the Chls *b*, including the bluest Chls *a*.[17] The calculated 5.1 ps component, however, accounts mostly for the equilibration among the Chls *a*, while the extra 1.4 ps component describes the equilibration between Chls *a* and the Chls *b*. The experimental 0.48 ps component appears to arise from the equilibration between the Chl *a* and *b* pools. The corresponding calculated 0.47 ps component does not account for the equilibration with the redmost Chls *a*, however, but it is complemented by an extra 0.31 ps component which describes that equilibration process. Obviously, such close-lying lifetimes would not be resolved experimentally. The additional significant component of 90 fs accounts for the pairwise equilibration mode between the bluest Chls *b* and *a* (645.3−664.9 nm; see Figure 2 and Table 3). This component is not resolved in the experiment (it may be buried in the coherent effects).

A direct judgment of fit quality can be obtained by comparison of the kinetic traces at various probe wavelengths as is actually done during the optimization procedure (see Figure 7). Given the multiexponential decay over a large dynamic range, the fitting time window was divided into five intervals with linear time grids (+0.05, −0.2, −1, −8, −15, and +4000 ps; 20 points per interval). Poor fits are found on the wings of the LHC II absorption spectrum and in the region where the difference absorption is very small (around 660 nm) due to zero crossing of components. Irrespective of the reason for these still existing problems, fits could be much improved if (a) more experimental data at different excitation wavelengths were provided and (b) perhaps more importantly, if better individual model spectra were available. These will be important points for future modeling.

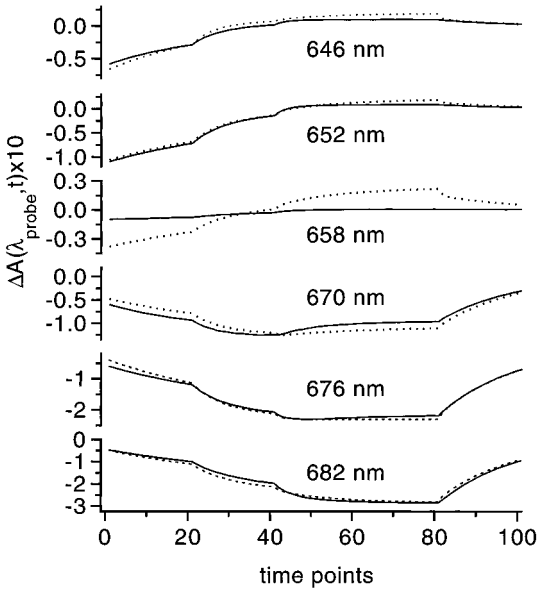

Figure 7. Comparison of the experimental and the calculated difference absorption time courses at several probe wavelengths for the free search model. Note that the time scale runs over five different time intervals in order to span the large time range and give sufficient resolution: +0.05; −0.2; −1.; −8.; −15.; −4000 ps; 20 equidistant time points were used for each interval.

It is important to note that no components substantially longer than 5 ps appeared in the simulations. In a recent LHC II transient absorption study[10] where measurements have been performed at 77 K, in addition to the lifetime discussed above, components on the time scale of 10−20 ps were reported. However, these components might either arise from partial excitation annihilation or from inhomogeneous broadening effects on the kinetics which cannot be ignored at the lower temperatures.[28] Both could give rise to such relatively slow components.

Trimer vs Monomer Kinetics. In the case of perfect symmetry, trimer and monomer kinetic component lifetimes are related for the discussed free search model as presented in Table 2 (see Figure 6a and also Table 3). The effect of intermonomer coupling (the participation of the intermonomer energy transfer) is almost negligible on all the equilibration components except for the longest one which reduces the lifetime from 6.6 to 5.1 ps in the trimer. Such a small reduction is due to a weak intermonomer coupling of the present optimal fit model. From the six closest intermonomer pairs of Chl molecules separated by less than 2 nm ($a4-a5'$, $a3-{}^{a}7'$, $a4-b5'$, $a5-a5'$, $a7-b3'$, $b2-b6'$) just the first one provides a significant contribution to the kinetics. The increase of intermonomer coupling, by providing more favorable orientations of Chls for faster intermonomer transfer, would much shorten the longest equilibration component lifetime while almost not affecting the amplitude spectra. This suggests that in this respect the model predictions could be tested easily in kinetic experiments by comparing the longest equilibration component lifetimes for monomeric and trimeric LHC II particles. A finding of small changes only in the longest equilibration component lifetime would support our model.

The absence of longer than a ∼5 ps equilibration kinetic components in the simulations gives a hint that the 34 and 85 ps components observed in the low-intensity transient absorption measurements[17] (see Figure 6b) are neither related to the excitation energy transfer in the intact LHC II monomer nor between monomers. One possibility might be that some annihilation occurred despite the low excitation density. We believe, however, that we can exclude this possibility (see ref

17). A further possibility is the presence of a small amount of higher oligomers or aggregates. Since the 35 ps component DADS is almost all negatively defined and its spectral shape is similar to the 3.6 ns component spectrum, this might indicate that some LHC II trimeric particles in the sample contain an energy acceptor (trap) in contact to the redmost Chls *a*. One red Chl (*b*1, 683 nm) is on the periphery of the complex and might be in contact to some unknown quencher. The amplitude of the 85 ps component is much lower and has the character of an equilibration component. This component might possibly originate from protein relaxation induced by the excited state dipoles (see ref 35).

We attempted in this work a detailed assignment of Chl molecules in LHC II. The recent analysis of multicolor transient absorption measurements of LHC II trimers at 77 K [10] is the only data set which can reasonably be compared with ours. However, inhomogeneous broadening effects, important at low temperatures but not taken into account explicitly in the analysis, make a detailed comparison difficult. These authors assumed the conventional Chl assignment. In spite of two swapped Chl *a* and *b* pairs in our optimal model, in general the overall energy transfer processes between the Chls in either assignment are quite similar. We note, however, that the optimal fitting for the two cases requires different dipole orientations, and consequently the two models have distinctly different LD spectra. From the present model one can in principle understand quite well which Chls and what time scales contribute to the various kinetic and spectral components.

Conclusions

A model of Chl *a* and *b* spectral type and transition dipole moment orientation distribution in LHC II structure[1] which satisfactorily reproduces the low-intensity femtosecond transient absorption as well as steady state data (fluorescence, LD) is obtained. It suggests a swap of two Chl *a* with Chl *b* locations as compared to Chl identities proposed up to now.[1] The modeling results suggest weak coupling between the Chls *a*, stronger coupling ($V \leq 100$ cm^{-1}) between the pairs of Chls *a* and *b* in the LHC II monomer and weak energy transfer coupling between the monomers in the trimer. This implies that to a first approximation energy transfer between Chls in LHC II is well-described by the Förster mechanism. Excitation energy equilibration is fast and the longest process takes about 5 ps in the trimer. Good agreement with the excitonic model[7] shows that the excitonic approach, when used to search for a fit to the steady state LD and CD spectra, converges to the weak Chl *a* coupling limit as well. This gives support to our approach in approximating the absorption spectrum of LHC II by a sum of noninteracting Chl spectra and the use of the Förster mechanism to describe the energy transfer kinetics. Despite this good agreement, we wish to note here explicitly that in order to explain more detailed experimental data it might well turn out that some limited exciton coupling has to be included into the model.

It is also important to note here that the fitness of the obtained best model of the experimental data[17] is presently not high enough to exclude all other, slightly different, models although the variations in location and spectral assignment of Chls are not expected to be large in further improved models. In order to test further the proposed model, both experimentally and theoretically, multiple excitation wavelength transient absorption data as well as more accurate steady state spectroscopic data and spectral decompositions are required.

Acknowledgment. The authors wish to acknowledge Prof. W. Kühlbrandt for providing structural coordinates for the LHC II pigments, Dr. L. Konermann for providing the spectral deconvolution program, and Dr. H van Amerongen for helpful discussion. This work was supported in part by the Bundesministerium für Bildung, Wissenschaft, Forschung und Technologie, Bonn, Germany (Project No. 0311206); the Deutsche Forschungsgemeinschaft (Sonderforschungsbereich 189, Heinrich-Heine-Universität Düsseldorf); and the Max-Planck-Institut für Strahlenchemie (visiting grant to G.T.). Financial support from the European Community (Human Capital and Mobility) to J.P.C. is also acknowledged. We also acknowledge Prof. K. Schaffner for support.

Appendix A

The incoherent excitation dynamics in the LHC II trimeric particle consisting of N pigments is described by the Pauli master equation

$$\dot{P}_i(t) = \sum_j T_{ij} P_j(t) \tag{A1}$$

where $P_i(t)$ stands for the occupation at time t of the excited state of pigment i. T_{ij} is the transfer rate matrix with elements

$$T_{ij} = (w_{ij} - \delta_{i,j}(w_{ij} + \sum_n w_{ni} + k_{0j}) \tag{A2}$$

where k_{0j} stands for the nonradiative decay rate of pigment j. The downhill and uphill energy transfer rates satisfy the detailed balance relation

$$w_{ji} = w_{ij} \exp(-(E_j - E_i)/k_B T) \tag{A3}$$

where k_B is the Boltzmann constant and T stands for the temperature. Assuming a C_3 symmetry of the LHC II monomer arrangement in a trimer, the submatrix structure of $\mathbf{T}$ is given by

$$\mathbf{T} = \begin{bmatrix} \mathbf{a} & \mathbf{b} & \mathbf{c} \\ \mathbf{c} & \mathbf{a} & \mathbf{b} \\ \mathbf{b} & \mathbf{c} & \mathbf{a} \end{bmatrix} \tag{A4}$$

where submatrix $\mathbf{a}$ stands for the intramonomeric transfer matrix and submatrices $\mathbf{b}$ and $\mathbf{c}$ reflect the intermonomer transfer. A similarity transformation applied to $\mathbf{T}$ by use of a transformation matrix $\mathbf{C}$ composed from the C_3 group character table[30]

$$\mathbf{C} = \begin{bmatrix} c_1 & c_2 & c_2 \\ c_1 & c_2\epsilon & c_2\epsilon \\ c_1 & c_2\epsilon^* & c_2\epsilon \end{bmatrix} \tag{A5}$$

where $c_1 = 1/(3)^{1/2}$ and $c_2 = 1/(1 + \epsilon^2 + (\epsilon^*)^2)^{1/2}$ and the asterisk means the complex conjugate, results in the block diagonal matrix

$$\mathbf{T'} = \mathbf{C}^{-1}\mathbf{T}\mathbf{C} = \begin{bmatrix} \mathbf{a}+\mathbf{b}+\mathbf{c} & \mathbf{0} & \mathbf{0} \\ \mathbf{0} & \mathbf{a} - [(\mathbf{b}+\mathbf{c})/2] + i\sqrt{3}[(\mathbf{b}-\mathbf{c})/2] & \mathbf{0} \\ \mathbf{0} & \mathbf{0} & \mathbf{a} - [(\mathbf{b}+\mathbf{c})/2] - i\sqrt{3}[(\mathbf{b}-\mathbf{c})/2] \end{bmatrix} \tag{A6}$$

As long as we simulate isotropic decay data, we are interested only in the occupations summed over all symmetrically equivalent pigment. Thus, the problem of finding the solution for eq

A1 for the LHC II trimer reduces to solving the eigenvalue problem for the renormalized monomeric transfer matrix **a** + **b** + **c**.[31]

Appendix B

To a more precise estimate of the short-time excitation evolution in a degenerate dimer, we use the stochastic Liouville equation approach.[23] In the high-temperature limit it results in a pair of kinetic equations for the density matrix element combinations:

$$\dot{p} = 2iVr - 2w_{12}p$$

$$\dot{r} = 2iVp - 2\Gamma r \qquad \text{(B1)}$$

where p and r stand for the difference between the diagonal and off-diagonal density matrix elements, respectively: $p = \rho_{11} - \rho_{22}$; $r = \rho_{12} - \rho_{21}$; V is the energy of interpigment electronic coupling; w_{12} equals approximately a Förster transfer rate between the pigments in a dimer. The Γ originates from the electron−vibration coupling and is mainly related to the local fluctuations of the monomeric excitation energies. In the estimations we relate Γ roughly to a thermal fluctuation energy. A purely incoherent energy transfer case is recovered by taking $V = 0$ in eq B1.

Appendix C

The reduced linear dichroism spectrum is defined as[32]

$$D^{L}(\lambda) = \frac{A_{\perp}(\lambda) - A_{||}(\lambda)}{A_{\perp}(\lambda) + 2A_{||}(\lambda)} \qquad \text{(C1)}$$

where $A_{\perp}$ and $A_{||}$ stand for the absorption of light with polarization perpendicular and parallel, respectively, to the trimeric plane. For the assumed axially symmetric trimers deposited as disks in the xy plane

$$A_{\perp}(\lambda) = kx\sum_i A_i(\lambda)\langle(\vec{e}_z,\vec{\mu}_i)^2\rangle = kx\sum_i A_i(\lambda)(\vec{\mu}_i{}^z)^2 \qquad \text{(C2)}$$

where k is a factor depending on the concentration of pigments in the sample; x is the sample thickness; $\vec{e}_z$ is a unit vector in the direction of perpendicular polarization; $\vec{\mu}_i$ and Ai(λ) are the transition dipole moment unit vector and the absorption spectrum of pigment i, respectively. In eq C2 $\vec{\mu}_i{}^z$ stands for projection of the transition dipole moment to the trimeric symmetry (Z) axis.

$$A_{||}(\lambda) = kx\sum_i A_i(\lambda)\langle(\vec{e}_{xy},\vec{\mu}_i)^2\rangle = \frac{1}{2}kx\sum_i A_i(\lambda)[(\vec{\mu}_i{}^x)^2 + (\vec{\mu}_i{}^y)^2] \qquad \text{(C3)}$$

where the expression in brackets stands for the transition dipole moment projection to the trimer (xy) plane and the factor $^1/_2$ derives from the average over all the transition dipole directions in the xy plane. The substitution of eqs C2 and C3 into eq C1 results in

$$D^{L}(\lambda) = \sum_i A^n{}_i(\lambda)\left[(\vec{\mu}_i{}^z)^2 - \frac{1}{2}(\vec{\mu}_i{}^x)^2 - \frac{1}{2}(\vec{\mu}_i{}^y)^2\right] \qquad \text{(C4)}$$

where $A^n{}_i(\lambda)$ stands for the normalized absorption spectrum

$$A^n{}_i(\lambda) = \frac{A_i(\lambda)}{\sum_i A_i(\lambda)} \qquad \text{(C5)}$$

Values of the reduced LD calculated using eqs C1−C5 are directly comparable with experimentally determined data given in Table 1 of ref 29 which are also plotted in Figure 3 of this paper.

References and Notes

(1) Kühlbrandt, W.; Wang, D. N.; Fujiyoshi, Y. *Nature* **1994**, *367*, 614.
(2) Jennings, R. C.; Bassi, R.; Zucchelli, G. *Top. Curr. Chem.* **1996**, *177*, 147.
(3) Jansson, S. *Biochim. Biophys. Acta* **1994**, *1184*, 1.
(4) Ruban, A. V.; Young, A. J.; Horton, P. *Biochemistry* **1996**, *35*, 674.
(5) Peterman, E. J. G.; Dekker, F. M.; van Grondelle, R.; van Amerongen, H. *Biophys. J.* **1995**, *69*, 2670.
(6) Nussberger, S.; Dekker, J. P.; Kühlbrandt, W.; van Bolhuis, B. M.; van Grondelle, R.; Van Amerongen, H. *Biochemistry* **1994**, *33*, 14775.
(7) Gülen, D.; van Grondelle, R.; Van Amerongen, H. In *Photosynthesis*: *From Light to Biosphere*; Mathis, P., Ed.; Kluwer: Dordrecht, The Netherlands, 1995; Vol. 1, p 335.
(8) Du, M.; Xie, X.; Mets, L.; Fleming, G. R. *J. Phys. Chem.* **1994**, *98*, 4736.
(9) Bittner, T.; Irrgang, K.-D.; Renger, G.; Wasielewski, M. R. *J. Phys. Chem.* **1994**, *98*, 11821.
(10) Visser, H. M.; Kleima, F. J.; van Stokkum, I. H. M.; van Grondelle, R.; Van Amerongen, H. *Chem. Phys.* **1996**, *210*, 297.
(11) Eads, D. D.; Castner, E. W.; Alberte, R. S.; Mets, L.; Fleming, G. R. *J. Phys. Chem.* **1989**, *93*, 8271.
(12) Palsson, L. O.; Spangfort, M. D.; Gulbinas, V.; Gillbro, T. *FEBS Lett.* **1994**, *339*, 134.
(13) Bittner, T.; Wiederrecht, G. P.; Irrgang, K.-D.; Renger, G.; Wasielewski, M. R. *Chem. Phys.* **1995**, *194*, 311.
(14) Kwa, S. L. S.; Van Amerongen, H.; Lin, S.; Dekker, J. P.; van Grondelle, R.; Struve, W. S. *Biochim. Biophys. Acta* **1992**, *1102*, 202.
(15) Mullineaux, C. W.; Pascal, A. A.; Horton, P.; Holzwarth, A. R. *Biochim. Biophys. Acta* **1993**, *1141*, 23.
(16) Valkunas, L.; Trinkunas, G.; Liuolia, V.; Van Grondelle, R. *Biophys. J.* **1995**, *69*, 1117.
(17) Connelly, J.; Müller, M. G.; Hucke, M.; Gatzen, G.; Mullineaux, C. W.; Horton, P.; Holzwarth, A. R. *J. Phys. Chem. B* **1997**, *101*, 1902.
(18) Connelly, J.; Müller, M. G.; Bassi, R.; Croce, R.; Holzwarth, A. R. *Biochemistry* **1997**, *36*, 281.
(19) Trinkunas, G.; Holzwarth, A. R. *Biophys. J.* **1994**, *66*, 415.
(20) Trinkunas, G.; Holzwarth, A. R. *Biophys. J.* **1996**, *71*, 351.
(21) Kühlbrandt, W.; Wang, D. N. *Nature* **1991**, *350*, 130.
(22) Hemelrijk, P. W.; Kwa, S. L. S.; van Grondelle, R.; Dekker, J. P. *Biochim. Biophys. Acta* **1992**, *1098*, 159.
(23) Rahman, T. S.; Knox, R. S.; Kenkre, V. M. *Chem. Phys.* **1979**, *44*, 197.
(24) Shipman, L. L.; Cotton, T. M.; Norris, J. R.; Katz, J. J. *J. Am. Chem. Soc.* **1976**, *98*, 8222.
(25) Lichtenthaler, H. K. *Methods Enzymol.* **1987**, *148*, 350.
(26) Becker, M.; Nagarajan, V.; Parson, W. W. *J. Am. Chem. Soc.* **1991**, *113*, 6840.
(27) Holland, J. H. *Adaptation in Natural and Artificial Systems*; MIT Press: Cambridge, MA, 1992.
(28) Konermann, L.; Gatzen, G.; Holzwarth, A. R. *J. Phys. Chem. B* **1997**, *101*, 2933.
(29) Van Amerongen, H.; Kwa, S. L. S.; van Bolhuis, B. M.; van Grondelle, R. *Biophys. J.* **1994**, *67*, 837.
(30) Cotton, F. A. *Chemical application of group throry*; Wiley: New York, 1990.
(31) Suter, G. W.; Holzwarth, A. R. *Biophys. J.* **1987**, *52*, 673.
(32) Van Gurp, M.; van Ginkel, G.; Levine, Y. K. *J. Theor. Biol.* **1988**, *131*, 333.
(33) Scherer, P. O. J.; Fischer, F. *Chem. Phys.* **1989**, *131*, 115.
(34) Gulbinas; *et al*. To be published.
(35) Trinkunas, G.; Holzwarth, A. R. *J. Phys. Chem. B* **1997**, *101*, xxxx.